Int. J. Heat Mass Transfer. Vol. 35, No. 7, pp. 1743–1751, 1992
Printed in Great Britain

0017 9310/92 $5.00 + 0.00

Rate of evaporation of water into superheated steam and humidified air

R. SHEIKHOLESLAMI and A. P. WATKINSON
Department of Chemical Engineering, The University of British Columbia, Vancouver, B.C., Canada V6T 1W5

(*Received* 9 *March* 1990 *and in final form* 21 *June* 1991)

Abstract—This paper examines the effect of steam content on the rate of evaporation of water into humid air and superheated steam at elevated temperatures. Experimental data on wood residue drying confirm the existence of an inversion point temperature above which the rate of evaporation of water increases with increases in the steam content of the medium. The process which is involved is theoretically confirmed through fundamental studies.

INTRODUCTION

THE DRYING process and a substantial number of other chemical engineering operations are involved with humidification or dehumidification of a gas phase. Air is the traditional drying medium; however, superheated steam drying is also practised [1]. Recycle and utilization of exit boiler flue gases or other humid process streams for the drying process, as a measure to reduce industrial energy expenditure, is also gaining more attention. The advantages of steam drying in comparison with air drying have been discussed [2–5]. The rate of the drying process is greatly affected by the steam content of the drying medium and that necessitates a more thorough understanding of the processes involved.

Wetted wall columns are traditionally used to investigate the rate of mass transfer between a gas and an evaporating surface. In drying solids of identical properties, size and shape, the rate of removal of free moisture during the constant drying rate period (R_{max}) can also approximate the effect of different variables on mass transfer within the gas phase. A number of batch drying experiments on Western Hemlock wood residues known as hog fuel (mainly bark) are used to examine the effect of humidity on the rate of evaporation of water from a fully saturated surface during the constant drying rate period.

EXPERIMENTAL WORK

The experiments were carried out [6] in a drying chamber which consists of an 8 in. schedule 10 stainless steel pipe (i.d. = 20.8 cm, o.d. = 21.9 cm) on batches of 3 kg wet hog fuel (58% wet basis moisture content) having a Sauter mean thickness of 6.3 mm. The apparatus was constructed to provide superheated steam, flue gas and humidified air as the drying media and to permit measurement of the drying rate of hog fuel under a range of conditions. Drying rates were determined through measurement of the change in humidity of the drying gas across the bed of hog fuel using an optical dew point sensor. For drying in superheated steam the drying rate was calculated from inlet and outlet mass flows measured by an orifice plate connected to a mass flow transmitter. Figure 1 represents a typical drying rate curve.

RESULTS AND DISCUSSION

Figure 2 depicts the effect of temperature on both superheated steam drying and air drying for a mass velocity of 142 kg h^{-1} (4383 kg m^{-2} h^{-1}). As the plot shows, the maximum drying rate is much higher with superheated steam than with relatively dry air at temperatures above approximately 180°C while the relationship is reversed below this point. Several

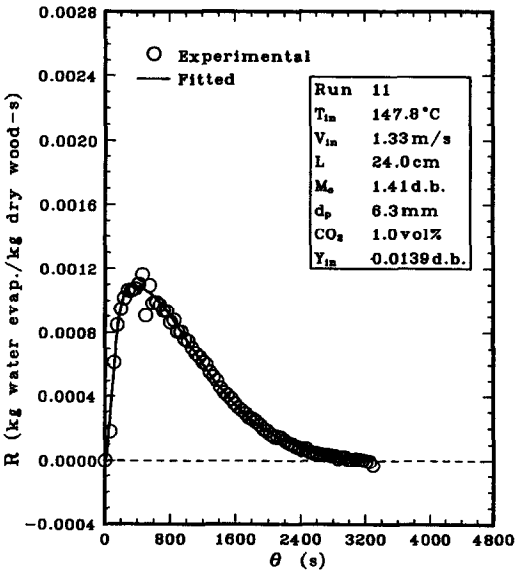

FIG. 1. A typical drying rate curve.

NOMENCLATURE

a_k	constants in equations (22) and (23)
A_i	interfacial surface area [m^2]
B	second virial coefficient [m^3 kmol^{-1}]
c_p	mean specific heat [J kg^{-1} K^{-1}]
C_l	specific heat of the liquid [J kg^{-1} K^{-1}]
Cs	specific heat per unit dry air [J kg^{-1} K^{-1}]
d_p	Sauter mean thickness [mm]
f	spline function of $\tilde{H}_{vap}$ [J kg^{-1}]
G_a	superficial mass flow of dry air [kg m^{-2} s^{-1}]
h	heat transfer coefficient [W m^{-2} K^{-1}]
H	enthalpy per unit dry gas [J kg^{-1}]
H'	enthalpy of mixture or steam [J kg^{-1}]
$\tilde{H}'$	molar enthalpy [J kmol^{-1}]
k_Y	mass transfer coefficient [kg m^{-2} s^{-1}]
L	bed height [cm]
m	mass flow rate [kg s^{-1}]
m_a	mass flow of dry air [kg s^{-1}]
n_t	total moles in a mixture [kmol]
N	rate of evaporation [kg s^{-1}]
p	pressure [Pa]
p_c	critical pressure [Pa]
p_s	saturation pressure at $T_r = 0.7$ [Pa]
p_r	reduced pressure
p_t	total pressure [Pa]
p_v	vapour pressure [Pa]
Q_{evap}	heat flow for evaporation [W]
R_g	gas constant [J kmol^{-1} K^{-1}]
R_{max}	rate during constant rate period [s^{-1}]
$\tilde{R}'(T)$	residual function of mixture [J kmol^{-1}]
$R(T)$	residual function per unit dry gas [J kg^{-1}]
St	Stanton number, (h/G_aCs)
T	temperature [°C or K]
T_b	boiling point of water [°C or K]
T_c	critical temperature [K]
T_r	reduced temperature
$\tilde{v}_g$	molar volume of the gas [m^3 kmol^{-1}]
$\tilde{v}_l$	molar volume of the liquid [m^3 kmol^{-1}]
V	velocity [m s^{-1}]
W	acentric factor
x_{ij}	constant in Table 1
Y	dry basis humidity [kg water/kg dry air]
Y'	mass fraction [kg water/kg mixture]
$\tilde{Y}'$	mole fraction [kmol water/kmol mixture].

Greek symbols

λ	latent heat of vaporization [J kg^{-1}]
$\tilde{\lambda}$	molar latent heat of vaporization [J kmol^{-1}].

Subscripts

a	dry air
as	adiabatic saturation
c	critical
db	dry bulb
i, j	unlike molecules in a binary mixture
in	inlet
k	0, 1 or 2
max	maximum
r	reduced
ref	reference, $T_{ref} = 0$°C
st	steam
t	total gas mixture
vap	water vapour.

experiments were carried out to see the effect of humidity on the rate of evaporation at elevated temperatures (202°C). The results (Fig. 3) are indicative of a drop in R_{max} with decreases in humidity.

These results are in good agreement with the reported values of Yoshida and Hyodo [7] on evaporation of water from a wetted-wall column into air, humid air and superheated steam. These authors [7] indicated that at elevated temperatures the rate of evaporation of water is higher into superheated steam than into dry air. They also noted that, at a given mass velocity, there is a temperature (inversion point) at which the evaporation rate is independent of the humidity of the drying gas. It was indicated that at temperatures lower than the inversion point the rate of evaporation decreases with increasing humidity while at temperatures above this point the reverse relationship prevails. The values of 170°C and 176°C were respectively reported for mass flow rates of 18 200 and 9100 kg m^{-2} h^{-1} and it was suggested that 'further investigation of the inversion point is necessary to make clear theoretically the reasons for its existence'.

This behaviour has been experimentally confirmed by other experimenters and the effects of other parameters such as gas mass flow rate, system geometry, hydrodynamics of the flow and different modes of energy transport on the inversion point temperature have also been investigated [8, 9]. Nomura and Hyodo [8] have considered convection to be the only process by which energy transport takes place and they calculated the inversion point for a flat plate and a sphere using the Pohlhausen and the Ranz and Marshall equations, respectively, to determine the convective heat transfer coefficient. Their calculations showed that under the purely convective mode of heat transfer the inversion point temperature was at 260°C and was independent of the gas mass velocity. However, the rate of heat transfer in the presence of a radiating gas (water vapour) is only partially dependent on the hydrodynamics of the flow. Therefore, considering the contributions made by the radiative component

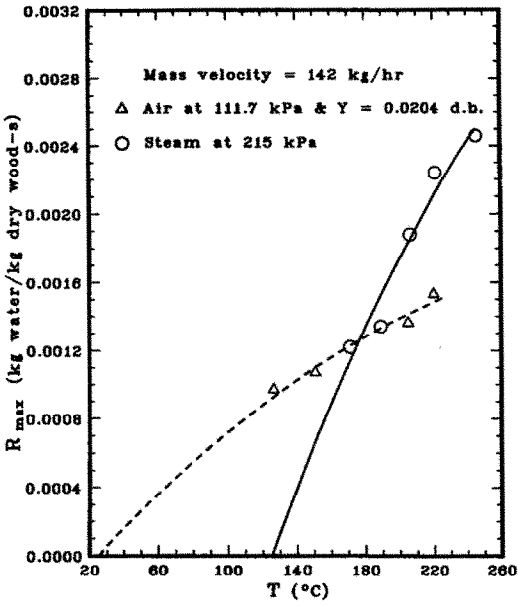

FIG. 2. Maximum drying rate vs temperature in air and steam.

of heat transfer and assuming that all constituents of the drying gas but dry air emit radiant heat, they modified their results and obtained an inversion temperature of approximately 200°C for a gas velocity of 30 000 kg m^{-2} h^{-1}. Their calculations indicated that the inversion point temperature decreased as the gas velocity was lowered and the relative effect of radiant heat becomes more predominant. This, however, is in contradiction with the experimental results of Yoshida and Hyodo [7] in a wetted-wall column. Faber *et al.* [9], in drying 1.63 mm alumina particles in a fluidized bed, also found an inversion temperature of 160°C for completely dry air and steam at the same mass flow. They calculated the same value by

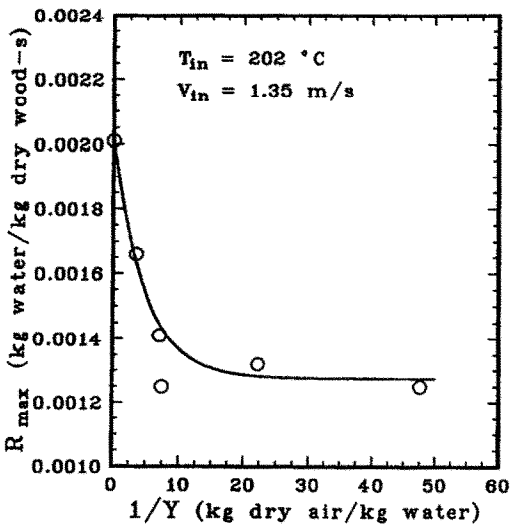

FIG. 3. Maximum drying rate vs absolute humidity.

using the definition of the inversion point (equal heat flows for both drying media) and considering a thermal equilibrium between the bed and the exit gas which exists under hydrodynamics of fluidization. Faber *et al.* [9] suggested 'more detailed work on the inversion temperature is required'.

The above-mentioned methods have been used for prediction of an inversion point temperature; however, no theoretical explanation for its existence and its locus with humidity has yet been given. The following discussion is an attempt to carry out that task from a thermodynamics point of view in two steps.

(i) The reason for the existence of an inversion point temperature is given through a comparison between heat transfer potential of superheated steam and air.

(ii) Considering that the slope of the adiabatic saturation lines on the psychrometric chart and the Stanton number at a given mass flow rate (m) are constant, the Number of Transfer Units is only a function of interfacial surface area (A_i). Therefore, for geometrically identical systems the fraction of maximum rate of evaporation (N/N_{max}) is only a function of A_i. For a given A_i and a given m, this necessitates the equality of N_{max} in both systems if equal rates of evaporation are required. Using this thermodynamic property of the air–water system, the locus of inversion point temperature with humidity is determined.

Since the drying process is accompanied by humidification of the drying gas, the evaporation process is first analysed to investigate the effect of humidity on the rate of drying. Consider the contact of a flow of gas at some temperature T_{db} and some partial pressure of water vapour $\bar{p}_{vap}$ with a fully wetted surface of a wood particle at temperature T_{as}. Equation (1) governs the maximum possible rate of evaporation of water into humid air. To facilitate the calculations, the wet bulb temperature is replaced by the adiabatic saturation temperature as they are the same for air–water mixtures. Since the evaporation of water into humid air would take place at wet bulb temperatures, any increase in air humidity would result in reduction of the thermal gradient ($T_{db}-T_{as}$) in addition to a drop in concentration gradient ($Y_{as}-Y_{db}$) and hence, it is believed, to lower the rate of evaporation at a given temperature

$$Q_{evap} = m_a(H_{as}-H_{db}) = m_a Cs(T_{db}-T_{as}) \quad (1)$$

$$c_{p_t} = \frac{c_{p_a}+Yc_{p_{vap}}}{1+Y} = \frac{Cs}{1+Y} \quad (2)$$

$$H = c_{p_a}(T-T_{ref})+Y[\lambda_{ref}+c_{p_{vap}}(T-T_{ref})]. \quad (3)$$

As it appears in equation (2), the heat capacity of the gas mixture, which is a function of the temperature, also increases with humidity to the extent represented by the following relationship:

$$\left(\frac{\partial c_{p_t}}{\partial Y}\right)_{T,p} = \frac{c_{p_{vap}} - c_{p_a}}{(1+Y)^2} \quad \text{for } 0 < Y < \infty \tag{4}$$

or

$$\left(\frac{\partial c_{p_t}}{\partial Y'}\right)_{T,p} = c_{p_{vap}} - c_{p_a} \quad \text{for } 0 < Y' < 1. \tag{5}$$

Therefore, an increase in humidity would result in two competing processes: a rise in specific heat which is counterbalanced by a rise in adiabatic saturation temperature and reduction of the thermal gradient.

To see the effect of humidity on the adiabatic saturation temperature at a given dry bulb temperature, the following set of equations should be solved simultaneously:

$$Cs(T_{db} - T_{as}) = (Y_{as} - Y_{db})\lambda_{as} \tag{6}$$

$$Y_{as} = \frac{18p_{v_{as}}}{29(p_t - p_{v_{as}})} \tag{7}$$

$$\ln p_{v_{as}} = \frac{-4986.667}{T_{as}} + 24.9 \quad T_{as} \text{ in K} \tag{8}$$

$$\lambda_{as} = c_{p_{vap}}(T_{as} - T_{ref}) + \lambda_{ref} - C_L(T_{as} - T_{ref}). \tag{9}$$

Equation (6) represents [10] an adiabatic saturation curve on the psychrometric chart. The intersection of this curve with the curve representing 100% saturation on the chart provides T_{as} at which the partial pressure of water vapour in the mixture equals the vapour pressure of the pure water at that temperature. Therefore, equation (7) defines the saturation absolute humidity (kg water/kg dry gas) at T_{as}. Assuming $\tilde{v}_l \ll \tilde{v}_g$ and applying the ideal gas law, the slope of the vapour pressure curve is related to the latent heat of evaporation [11] through

$$\frac{dp_v}{dT} = \frac{\tilde{\lambda} p_v}{R_g T^2}. \tag{10}$$

Integration of equation (10) over a narrow temperature range, where $\tilde{\lambda}$ can be considered constant [10], yields $\ln p_v$ as a linear function of $1/T$

$$\ln p_v = -\frac{\tilde{\lambda}}{R_g T} + A. \tag{11}$$

Equation (8) is obtained by substituting the numerical values of the vapour pressure of the water at two extremes of a given temperature range (20–100°C). Substitution of $p_{v_{as}}$ from equation (8) into equation (7) represents the equation of 100% saturation curve on the psychrometric chart. The latent heat of evaporation at adiabatic saturation temperature, λ_{as}, is formulated as a function of T_{as} and is given by equation (9). Therefore, simultaneous solution of equations (6)–(9) provides T_{as} as a function of both T_{db} and Y_{db} for 20°C < T_{as} < 100°C.

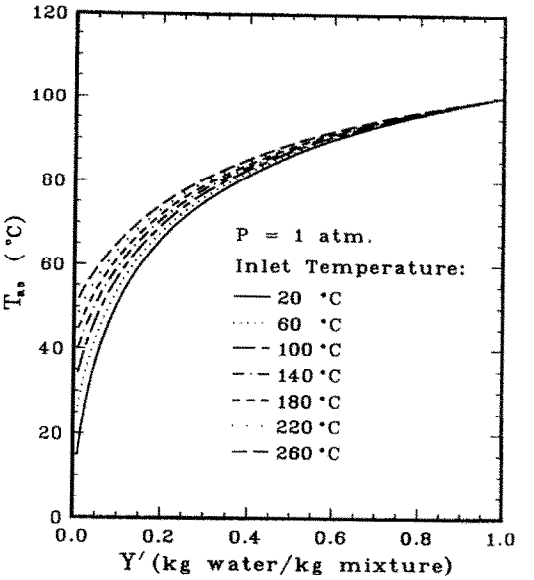

FIG. 4. Adiabatic saturation temperature as a function of humidity at various temperatures.

The results are plotted in Fig. 4 as adiabatic saturation temperature vs humidity for various inlet temperatures. As is shown, the saturation temperature rises asymptotically with humidity, therefore indicating that at a given temperature and high inlet humidities the magnitude of thermal gradient will be less affected by the rise in humidity. The asymptotic value is approached at much lower humidity values with increasing inlet temperatures. For instance, a saturation temperature of 60°C is expected for inlet humidity and temperature of, respectively, 0.154 kg water/kg mixture and 20°C. The same adiabatic temperature exists for a 260°C gas with an inlet humidity of 0.058 kg water/kg mixture.

A plot of mean specific heat capacity of the mixture is also prepared as a function of humidity at different temperatures and is shown in Fig. 5. The specific heat increases linearly with humidity to an extent given in equation (5) and, in comparison, it is very slightly affected by the inlet temperature. Figure 6 shows an increase in the maximum available enthalpy change in the gas with respect to temperature at a given humidity. The plot is indicative of the drop in heat capacity with humidity for a humidified gas compared to superheated steam below a certain temperature. The relationship is reversed above this temperature (*inversion temperature*) which itself decreases with humidity.

The above investigations, therefore, show that there exists a temperature where the evaporation of water is as fast in superheated steam as it is in humidified air. However, it does not provide us with a common inversion temperature at which evaporation is independent of humidity. To find the locus of the inversion point for different humidities, the following equation, which is based on the assumption of a fully saturated

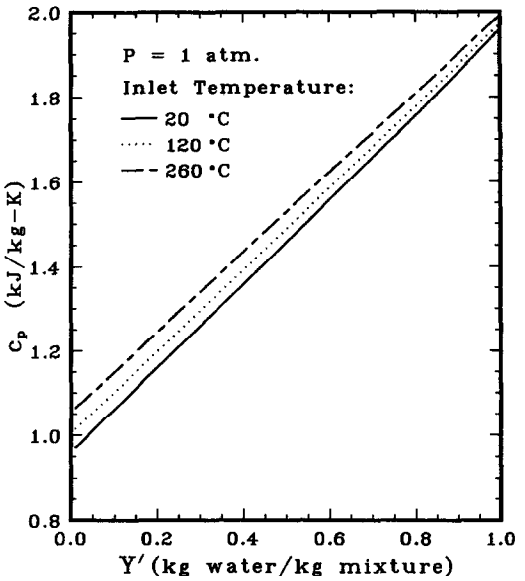

FIG. 5. Mean specific heat of the mixture vs humidity.

outcoming of either air or superheated steam at a constant mass flow rate, should be solved:

$$c_{p_{st}}(T-T_b) = c_{p_t}(T-T_{as}). \tag{12}$$

The above equation is solved simultaneously with equations (6)–(9) to get the inlet temperature where the evaporation rates are equal (*inversion point*) in superheated steam and air at a given air humidity. Figure 7 shows the locus of the inversion point as a function of air humidity at atmospheric pressure. The solid line on the plot indicates a value of 164°C for completely dry air which decreases with humidity,

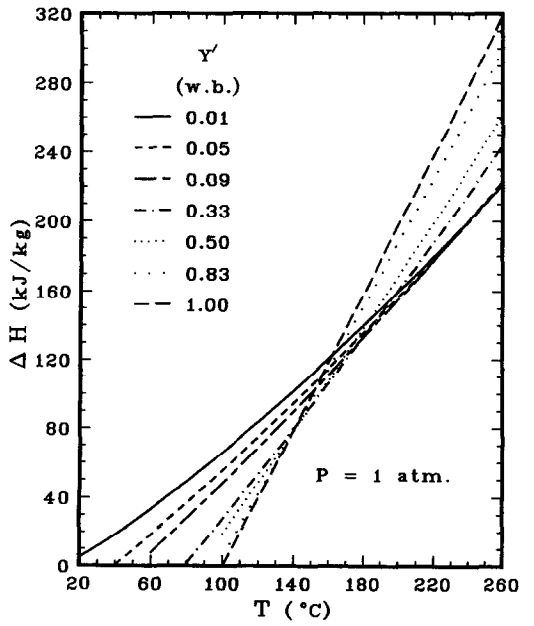

FIG. 6. Maximum change in gas enthalpy vs temperature at different humidities.

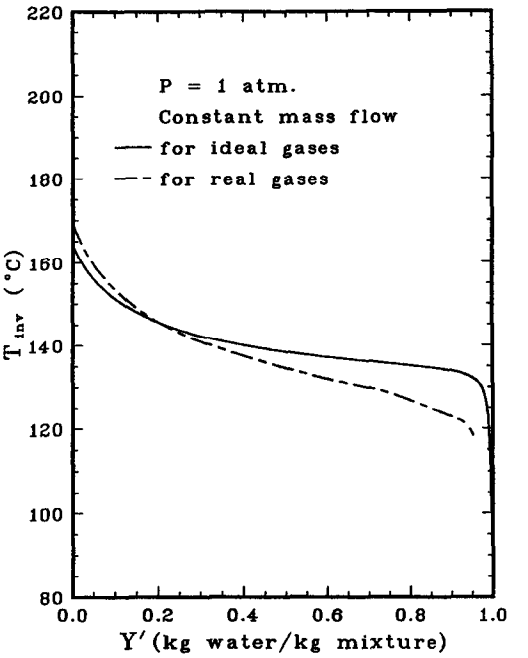

FIG. 7. Locus of inversion point vs humidity.

reaching a plateau at humidities above 0.1 kg water/kg total gas. As mentioned previously, the calculations have been carried out using the physical properties of both air and superheated steam at atmospheric pressure. The locus of inversion points is expected to shift up when superheated steam at higher pressures is used. Using the above procedure, an inversion point temperature of 189°C is obtained for superheated steam at 215 kPa and humidified air at $Y = 0.0204$ kg water/kg dry air and atmospheric pressure. This value is in very good agreement with the experimental results (Fig. 2) considering that the calculations are carried out for an ideal case of a uniform and fully saturated surface.

For ease of calculations, the gases are assumed to be ideal and the enthalpy only temperature dependent. However, the enthalpy of a real gas is a function of both temperature and pressure and the total change in that property is represented by the following expression:

$$dH' = \left(\frac{\partial H'}{\partial T}\right)_p dT + \left(\frac{\partial H'}{\partial p}\right)_T dp. \tag{13}$$

Using the following mathematical relationship which exists between the derivatives of a function $Z = f(X, Y)$:

$$\left(\frac{\partial Y}{\partial Z}\right)_X \left(\frac{\partial Z}{\partial X}\right)_Y \left(\frac{\partial X}{\partial Y}\right)_Z = -1 \tag{14}$$

we can write

$$dH' = \left(\frac{\partial H'}{\partial T}\right)_p dT - \left(\frac{\partial T}{\partial p}\right)_{H'} \left(\frac{\partial H'}{\partial T}\right)_p dp \tag{15}$$

where

$$c_p = \left(\frac{\partial H'}{\partial T}\right)_p \tag{16}$$

is the specific heat at constant pressure and

$$\mu = \left(\frac{\partial T}{\partial p}\right)_{H'} \tag{17}$$

is defined as the Joule–Thomson coefficient. Thus, equation (13) becomes

$$\mathrm{d}H' = c_p\,\mathrm{d}T - \mu c_p\,\mathrm{d}p. \tag{18}$$

As is seen in equation (17), μ relates the change in temperature with respect to pressure. A positive value for μ indicates that a drop in pressure has a cooling effect on the gas. For an ideal gas $\mu = 0$ while for almost all real gases—except H_2, Ne and He—at normal pressures and temperatures $\mu > 0$ and changes sign at high temperatures, or pressures as it goes toward the liquid state. Therefore, in the evaporation of water into air which is considered to be taking place under adiabatic conditions, the Joule–Thomson coefficient can be used to relate the changes of temperature with respect to pressure.

Equation (18) indicates that the less positive the Joule–Thomson coefficient, the higher would be the heat capacity of the gas. Substituting

$$p = p_{\mathrm{vap}} + p_{\mathrm{a}} \tag{19}$$

into equation (17) and rearranging would result in

$$\frac{1}{\mu} = \left(\frac{\partial p_{\mathrm{vap}}}{\partial T}\right)_{H'} + \left(\frac{\partial p_{\mathrm{a}}}{\partial T}\right)_{H'} \tag{20}$$

or

$$\frac{1}{\mu} = \left(\frac{1}{\mu}\right)_{\mathrm{vap}} + \left(\frac{1}{\mu}\right)_{\mathrm{a}}. \tag{21}$$

It is obvious that μ_{vap} is higher at low partial pressures of vapour. Also, at a given temperature the Joule–Thomson coefficient is lower for water than for air; therefore, the higher the partial pressure of the water the less positive would be the μ and hence the higher would be the heating capacity of the mixture.

In view of all which has been said above, it can be concluded that since the adiabatic saturation temperature of air at high dry bulb temperatures is not strongly affected by its water content and the specific heat of the air rises rapidly with the water content, the latter would be considered the controlling factor in the evaporation process. Therefore, thermodynamics indicates that at high temperatures, the higher the air humidity, the higher would be the potential for evaporation of water from a fully saturated surface.

As the properties of superheated steam at low degrees of superheat greatly deviate from the ideal gas, equations (6), (8), (9) and (12) were modified to more closely approximate the conditions for a real gas. Therefore, tabulated data [12] were used to determine the vapour pressure and latent heat as expressed by the following equations:

$$\ln p_{\mathrm{v}} = -\frac{a_0}{T} + a_1 \tag{22}$$

$$\lambda = \frac{R_{\mathrm{g}} T}{18}[a_2 + \ln p_{\mathrm{v}}]. \tag{23}$$

The enthalpy of superheated steam and gas mixture in equations (12) and (6) were respectively replaced by equations (24) and (25)

$$H'_{\mathrm{vap}} = f(T) \tag{24}$$

$$H = H'_{\mathrm{a}} + YH'_{\mathrm{vap}} + R(T) \tag{25}$$

where $f(T)$ is the spline function of the tabulated data [13] and $R(T)$ is the residual function taking into account the non-ideality of the mixture [12, 14]. The equations for $R(T)$, and for the corresponding real gas calculations of the inversion curve, are listed in Table 1. The variable x_{ij} represents the deviation of T_{cij} from the geometric mean of the critical temperatures of the pure substances, and its value becomes more positive as the difference in shape, size or chemical nature of the constituents increases. The experimental results reported [14] for several systems of binary mixtures generally indicate $0 \leqslant x_{ij} \leqslant 0.20$.

Table 1. Equations used for calculation of the enthalpy of a real gas mixture

$$R(T) = \frac{n_{\mathrm{t}}}{m_{\mathrm{a}}}\tilde{R}'(T)$$

$$= \frac{n_{\mathrm{t}}}{m_{\mathrm{a}}}\Delta\tilde{H}'$$

$$= pT\left[\frac{\mathrm{d}B}{\mathrm{d}T} - \frac{B}{T}\right]$$

$$B = \sum_i \sum_j \tilde{Y}'_i \tilde{Y}'_j B_{ij}$$

$$\frac{\mathrm{d}B}{\mathrm{d}T} = \sum_i \sum_j \tilde{Y}'_i \tilde{Y}'_j \frac{\mathrm{d}B_{ij}}{\mathrm{d}T}$$

$$B_{ij} = \frac{R_{\mathrm{g}} T_{cij}}{p_{cij}}[B^0 + W_{ij} B^1]$$

$$B^0 = 0.1445 - \frac{0.33}{T_{\mathrm{r}}} - \frac{0.1385}{T_{\mathrm{r}}^2} - \frac{0.0121}{T_{\mathrm{r}}^3}$$

$$B^1 = 0.073 + \frac{0.46}{T_{\mathrm{r}}} - \frac{0.5}{T_{\mathrm{r}}^2} - \frac{0.097}{T_{\mathrm{r}}^3} - \frac{0.0073}{T_{\mathrm{r}}^8}$$

$$W_{ii} = -\log p_{\mathrm{s}_{\mathrm{r}}} - 1.0$$

$$p_{\mathrm{s}_{\mathrm{r}}} = \frac{p_{\mathrm{s}}}{p_c} \quad \text{at } T_{\mathrm{r}} = 0.7$$

$$V_{cij} = \tfrac{1}{8}[V_{ci}^{1/3} + V_{cj}^{1/3}]^3$$

$$T_{cij} = (T_{ci} T_{cj})^{0.5}(1 - x_{ij})$$

$$Z_{ij} = 0.5(Z_i + Z_j)$$

$$Z_i = 1 + \frac{B_{ii} p}{R_{\mathrm{g}} T}$$

$$p_{cij} = \frac{Z_{ij} R_{\mathrm{g}} T_{cij}}{V_{cij}}$$

$$W_{ij} = 0.5(W_{ii} + W_{jj})$$

Due to the lack of data for the air–water system, x_{ij} values at both extremes were used for the calculation of T_{cij}; however, no appreciable effect on the inversion point temperature was obtained. Simultaneous solution of the above-mentioned equations generates the locus of the inversion point temperature for real gases as shown by the broken line in Fig. 7. It is evident that the trend of the inversion temperature with humidity is very similar for the ideal gas or the real gas situation.

The interactions of the mass and heat transfer processes during evaporation have been studied extensively. The convection heat transfer process is altered in the presence of liquid evaporation due to partial consumption of energy for sensible heating of evaporated moisture, and to the effects of evaporated moisture flow on both the hydrodynamics and thermodynamics of the evaporation process. The effects of sensible heating can be accounted for by the Ackerman coefficient, or by the methods of Kast [15] or Loo and Mujumdar [16]. The impacts of the cross flow of moisture on the turbulent boundary layer, and hence heat transfer are attributed [17–19] to wave formation, boundary layer thickening and entrainment of submicroscopic liquid particles. The conflicting reports on the effects of mass transfer on heat transfer are possibly due to combinations of the effects of the above processes.

The transport of moisture in drying with a superheated vapour is due to a pressure gradient between the solid surface and the bulk of the gas resulting in bulk flow of moisture. The wet surface is heated by the superheated steam until its temperature exceeds the saturation temperature of water at the system pressure by several degrees, which would provide enough of a pressure gradient to cause hydraulic movement of the evaporated moisture. Chu *et al.* [20] reported that a few hundredths of a degree is sufficient to provide bulk movement of water vapour, while Wenzel and White [21] reported that 1.5°C is required. Thus, at high drying temperatures, the surface temperature is rapidly raised causing the bulk flow to start at very early stages of drying.

For drying in air, the increase in the rate of evaporation with humidity seems to be in contradiction to the theoretically and widely accepted mass transfer law stating that the rate of transfer decreases as either the concentration or the vapour pressure gradient decreases. However, contrary to what might first seem apparent, the gradient for mass transfer also increases with humidity at high temperatures.

The instantaneous mass transfer flux between the gas and the saturated surface is represented by the following relationship:

$$N = k_Y(Y_{as} - Y_{db}). \tag{26}$$

Substituting equation (8) into equation (7) shows that the adiabatic saturation humidity is an exponential function of the saturation temperature. Therefore, for a very humid air with a high and relatively constant

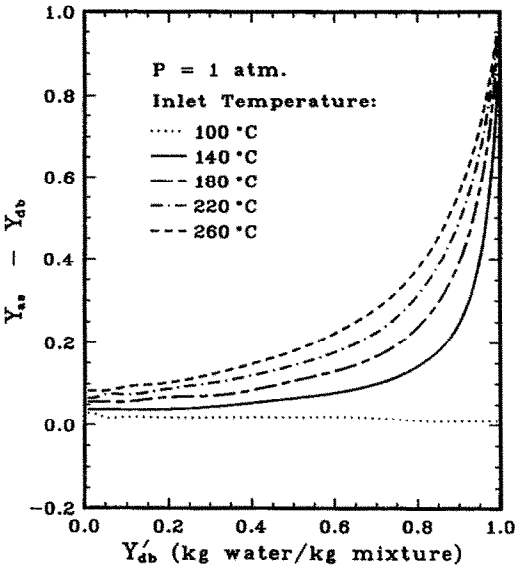

FIG. 8. Concentration gradient vs humidity at various temperatures.

adiabatic saturation temperature, even a small increase in the saturation temperature would greatly increase the saturation humidity and hence the concentration gradient $(Y_{as} - Y_{db})$. Figure 8 shows that the concentration gradient increases with humidity at temperatures above 100°C and the effect is much stronger at higher temperatures.

These results and equation (6) confirm the fact that at high temperatures the specific heat of the drying medium is the determining factor in the rate of the drying process. Also, contrary to what is generally thought, an increase in humidity of the gas is expected to increase the concentration gradient and hence the rate of evaporation of water, and result in a higher drying rate.

CONCLUSION

Batch drying experiments on Western Hemlock hog fuel confirmed the existence of an inversion point temperature. The data indicated that the drying rates during the heat transfer controlled period are higher in superheated steam than in relatively dry air ($Y = 0.0204$) at $T_{inv} > 180$°C, while the relationship is reversed at $T_{inv} < 180$°C. Drying experiments at $T = 202$°C were also indicative of an increase in the rates with increases in humidity. As the rate of drying during this period can approximate the rate of evaporation of water from a free surface, it can be concluded that the experimental results were in good agreement with the reported values [8] obtained from evaporation in a wetted-wall column.

The existence of the inversion point temperature is theoretically explained through the thermodynamics of the evaporating medium. The thermal gradient decreases with increases in humidity; however, at a given elevated temperature the main factor controlling

the rate of evaporation is the specific heat of the mixture, which is a linear function of the humidity of the drying medium. It is also theoretically shown that increases in the humidity at high temperatures increase the concentration gradient and, therefore, this phenomenon does not contradict the fundamental principles of mass transfer. The locus of the inversion point temperature is determined for both real and ideal gases.

Acknowledgements—The support of the Science Council of British Columbia and the Natural Sciences and Engineering Research Council of Canada is gratefully acknowledged.

REFERENCES

1. C. Beeby and O. E. Potter, Steam drying. In *Drying '85* (Edited by R. Toei and A. Mujumdar), pp. 41–58. Hemisphere, New York (1985).
2. M. Hasan, A. S. Mujumdar and M. Ai-Taleb, Laminar evaporation from flat surfaces into unsaturated and superheated solvent vapor. In *Drying '86* (Edited by A. Mujumdar), pp. 604–616. Hemisphere, New York (1986).
3. J. Meunier and R. J. Munz, Flash drying with superheated steam—a mathematical model. In *Drying '86* (Edited by A. Mujumdar), pp. 580–587. Hemisphere, New York (1986).
4. S. Hilmart and U. Gren, Steam drying of wood residues—an experimental study. In *Drying '87* (Edited by A. Mujumdar), pp. 210–217. Hemisphere, New York (1987).
5. C. Beeby and O. E. Potter, Heat transfer between a horizontal tube bundle and fine particles with air or steam, *A.I.Ch.E. Jl* **30,** 977–980 (1984).
6. R. Sheikholeslami, Drying of hog fuel in a fixed bed, Ph.D. thesis, Special Collections, Main Library, University of British Columbia, Vancouver (1990).
7. T. Yoshida and T. Hyodo, Evaporation of water in air, humid air, and superheated steam, *Ind. Engng Chem. Process. Des. Dev.* **9,** 207–214 (1970).
8. T. Nomura and T. Hyodo, Behaviour of inversion point temperature and new applications of superheated steam vapour drying. In *Drying '85* (Edited by R. Toei and A. Mujumdar), pp. 517–522. Hemisphere, New York (1985).
9. E. F. Faber, M. D. Heydenrych, R. U. I. Seppä and R. E. Hicks, A techno-economic comparison of air and steam drying. In *Drying '86* (Edited by A. Mujumdar), pp. 588–594. Hemisphere, New York (1986).
10. R. E. Treybal, *Mass-transfer Operations* (3rd edn), Chemical Engineering Series. McGraw-Hill, New York (1980).
11. M. D. Burghardt, *Engineering Thermodynamics with Applications* (2nd edn). Harper & Row, New York (1982).
12. R. H. Perry and C. H. Chilton, *Chemical Engineers' Handbook* (5th edn), pp. 4-56–4-68. McGraw-Hill, New York (1973).
13. H. Lester, J. S. Gallagher and G. S. Kell, *NBS/NRC Steam Tables*. Hemisphere, New York (1984).
14. J. M. Prausnitz, R. N. Lichtenthaler and E. G. de Azevedo, *Molecular Thermodynamics of Fluid-phase Equilibria* (2nd edn), Chapters 4 and 5. Prentice-Hall, Englewood Cliffs, NJ (1986).
15. W. Kast, Coefficients for the combined heat and momentum transfer in laminar and turbulent boundary layers. In *Proc. 7th Int. Heat Transfer Conf.*, Vol. 3, pp. 263–268. Hemisphere, New York (1982).
16. E. Loo and A. S. Mujumdar, A simulation model for combined impingement and through drying using superheated steam as the drying medium. In *Drying '84* (Edited by A. Mujumdar), pp. 264–280. Hemisphere, New York (1984).
17. B. M. Smolsky, Heat and mass transfer with liquid evaporation. In *Progress in Heat and Mass Transfer*, Vol. 4, pp. 97–107. Pergamon Press, New York (1971).
18. B. M. Smolsky and G. T. Sergeve, Heat and mass transfer with liquid evaporation, *Int. J. Heat Mass Transfer* **5,** 1011–1021 (1962).
19. G. F. Hewitt and A. H. Govan, Phenomenological modelling of non-equilibrium flows with phase change, *Int. J. Heat Mass Transfer* **33,** 229–242 (1990).
20. C. J. Chu, A. M. Lane and D. Conklin, Evaporation of liquids into their superheated vapors, *Ind. Engng Chem.* **45,** 1586–1591 (1953).
21. L. Wenzel and R. R. White, Drying granular solids in superheated steam, *Ind. Engng Chem.* **43,** 1829–1837 (1951).

VITESSE D'EVAPORATION DE L'EAU DANS LA VAPEUR SURCHAUFFEE ET DANS L'AIR HUMIDE

Résumé—On examine l'effet du contenu de vapeur d'eau sur la vitesse d'évaporation de l'eau dans l'air humide et dans la vapeur surchauffée aux températures élevées. Des expériences sur le séchage de résidus de bois confirment l'existence d'une température de point d'inversion au-dessous de laquelle la vitesse d'évaporation de l'eau augmente avec l'accroissement du contenu de vapeur d'eau du milieu. Le mécanisme concerné est théoriquement confirmé par des études fondamentales.

DIE VERDAMPFUNGSGESCHWINDIGKEIT VON WASSER IN ÜBERHITZTEN DAMPF UND FEUCHTE LUFT

Zusammenfassung—In der vorliegenden Arbeit wird der Einfluß des Dampfanteils auf die Verdampfungsgeschwindigkeit von Wasser in feuchte Luft und überhitzten Dampf bei erhöhten Temperaturen untersucht. Versuchsergebnisse über die Trocknung von Holzresten bestätigen die Existenz einer Inversions-Punkt-Temperatur, oberhalb der die Verdampfungsgeschwindigkeit von Wasser mit steigendem Dampfanteil im Medium zunimmt. Der gesamte Vorgang wird theoretisch durch grundlegende Untersuchungen bestätigt.

СКОРОСТЬ ИСПАРЕНИЯ ВОДЫ В ПЕРЕГРЕТЫЙ ПАР И ВЛАЖНЫЙ ВОЗДУХ

Аннотация—Исследуется влияние паросодержания на скорость испарения воды во влажный воздух и перегретый пар при высоких температурах. Экспериментальные данные по сушке древесных остатков подтверждают существование температуры инверсии, выше которой скорость испарения воды возрастает с увеличением паросодержания среды. Рассматриваемый процесс теоретически подтверждается фундаментальными исследованиями.